

Monotonic and Cyclic Behavior of Chiang Mai Sand Under Simple Shear Mode

Soksan Thay · Suched Likitlersuang ·
Thirapong Pipatpongsa

Received: 18 April 2012 / Accepted: 1 October 2012 / Published online: 20 October 2012
© Springer Science+Business Media Dordrecht 2012

Abstract Record of damages and casualties caused by earthquakes in Thailand reveals that Chiang Mai, the second largest province of Thailand, has faced the great threat among other provinces. Triaxial tests, standard penetration tests, and multichannel analysis of surface wave have been recently performed to understand the dynamic response of Chiang Mai ground. However, the cyclic simple shear test, which could convincingly represent the real seismic ground shaking under repeated horizontal shear force, has not been conducted yet. Therefore, this paper aims to characterize the behaviors of Chiang Mai sand under monotonic and cyclic loadings using a direct simple shear apparatus. Sand specimens taken from the Ping

River were prepared by dry deposition technique. The mobilized friction angle at the critical state measured by the direct simple shear test is equal to 37.3° which is 9 % less than that measured by direct shear box test. This paper also provides the appropriate dynamic properties of Chiang Mai sand with the shear strain level $<2\%$ for any practical purpose. Test results showed that the normalized shear modulus agrees well with other investigators while the damping ratio is noticeably smaller than the lower-bound range for sand reported in the past studies.

Keywords Damping · Direct shear test · Dynamic · Hysteresis · Shear strength

S. Thay
Department of International Development Engineering,
Tokyo Institute of Technology, 2-12-1-17-2 O-okayama,
Meguro-ku, Tokyo 152-8550, Japan
e-mail: soksan007@yahoo.com

S. Likitlersuang (✉)
Department of Civil Engineering, Faculty of Engineering,
Chulalongkorn University, Phayathai Rd., Pathumwan,
Bangkok 10330, Thailand
e-mail: fceslk@eng.chula.ac.th

T. Pipatpongsa
Global Scientific Information and Computing Center,
Tokyo Institute of Technology, 2-12-1-17-2 O-okayama,
Meguro-ku, Tokyo 152-8550, Japan
e-mail: pthira@gsic.titech.ac.jp

1 Introduction

The recent record of major earthquakes has become a major concern in Thailand. These temblors caused the destruction of the infrastructure system and some casualties. On 24 March 2011, the large 6.8 magnitude quake, whose epicenter was located in Burma, was felt in Thailand and resulted to devastation in the northern part, including Chiang Mai and Chiang Rai. Consequently, countermeasures for building and foundation design are required.

Gauchan (1984) conducted the undrained cyclic triaxial test to evaluate the liquefaction resistance of Chao Phaya sand taken from Bangkok, assuming some possible magnitudes of the induced earthquake.

Realizing the lack of historical seismic data, Nutalaya et al. (1985) created a database of seismicity in Thailand to pave the way for the induced earthquake assessment. The seismic hazard maps have been proposed to serve as guidelines for any practical purpose (Ornthammarath et al. 2011; Pailoplee et al. 2009). The active faults, which might induce medium earthquake, were specifically addressed in Northern Thailand. In addition, Teachavorasinskun et al. (2009) attempted to confirm the past investigations, focusing on the critical zone in Chiang Mai. An extensive data of standard penetration tests were collected to predict liquefaction potential of sand layers in Chiang Mai subsoil. Based on the in situ test data, they suggested that the potential of the earthquake in Chiang Mai province may provoke discernible destruction to the 2- or 3-storey buildings. Another nondestructive field test of multichannel analysis of surface wave was carried out by Seng (2008) to provide more seismic data throughout Thailand.

Although a number of seismic data in Thailand was considerably published for many decades, most of the data were obtained from the field tests and triaxial tests. According to Seed et al. (1986) the cyclic simple shear test convincingly represents the real seismic ground shaking under repeated horizontal shear force; however, this kind of test has not been conducted on Chiang Mai sand yet. The soil behavior can be well understood as long as there are many data from different laboratory tests. Therefore, the present study aims to characterize the dynamic properties (shear modulus and damping ratio) of Chiang Mai sand by a direct simple shear apparatus. The static sand properties in term of shear strength also briefly presents for additional information.

Since the behavior of soils strongly depends on strain, it is also necessary to determine the dynamic properties (shear modulus and damping ratio) of Chiang Mai sand at low shear strain amplitude. However, this is beyond the scope of the investigation reported herein, and will be left for future study. The results of this study would provide static and dynamic properties of Chiang Mai sand under simple shear mode for earthquake design and might be useful to provide robust design against various vibration sources such as pile driving, shallow compaction, blasting in demolition and mining, deep compaction by explosion, passing of trains and road vehicles, vehicle wheel drop into road holes and machinery

operations in regard to dynamic response of earth structures that meet the applied range of shear strain of the present study. Therefore, the results of the present study represent the dynamic characteristic of soil in the intermediate to large strain amplitude (shear strain of 0.5–2 %) and not small strain.

2 Interpretation of Soil Parameters from Direct Simple Shear Test

2.1 Background

After the clarification on concept of effective stress by Terzaghi in the early 1920s, many soil laboratory testing apparatuses (such as direct shear, direct simple shear, triaxial, and torsional shear apparatus, etc.) were invented to measure the shear strength of soil. Among them, the direct shear apparatus has been widely used both in research and application owing to the ease of operation, the low cost of expense, and the little time expenditure. However, the direct shear test consists of the disadvantages in terms of the deformation and stress distribution during shear. In accordance with Kjellman (1951), the deformation of the specimen in direct shear apparatus is non-uniform; it varies from one point to another point. This leads to the innovation of the direct simple shear apparatus which can overcome the deficiency in direct shear device. In direct simple shear machine, the deformation is approximately equal at all points and form an angle, namely “shear strain”. The distribution of stress is fairly good and certainly better than direct shear device, with reference to Kjellman (1951).

In Swedish Geotechnical Institute (SGI) direct simple shear apparatus, the cylindrical sample is used and completely surrounded by stack ring. Later, this apparatus’s design was modified by Bjerrum and Landva (1966) at the Norwegian Geotechnical Institute (NGI) using cylindrical sample confined by a wire-reinforced membrane. In this paper, NGI direct simple shear apparatus is employed to investigate the CM sand behavior.

2.2 Monotonic Direct Simple Shear Test

The direct simple shear test performed under plane strain condition in which the principal axes of stresses are free to rotate is related to stress state in many

practical geotechnical situations such as slope stability, embankment in accordance with Bjerrum and Landva (1966), and Roscoe (1970). The main advantages of this test are that the sample preparation and testing procedure are easy to perform. The strength parameters from this test can be interpreted by many researchers.

Budhu (1988), Ochiai (1981), Roscoe (1970), proposed various methods to interpret strength parameters from the direct simple shear test. Amongst these, the approach suggested by Roscoe (1970) has been commonly used assuming that the horizontal plane is a plane of failure, as depicted in Fig. 1; in which H_0 , γ , σ'_v , τ , δh and δv represent the initial height of specimen, shear strain, vertical effective stress, shear stress, horizontal displacement and vertical displacement after shearing respectively. This assumption can be considered reasonable both in constant volume or constant vertical stress condition, which is in agreement with other authors (Atkinson et al. 1991; Porcino et al. 2008). In this paper, the author follows the assumption by Roscoe (1970) to interpret the experimental results from the NGI direct simple shear test.

The shearing resistance along the horizontal failure plane from the direct simple shear test can be expressed as

$$\tau = \sigma'_v \tan \phi' + c \tag{1}$$

where σ'_v , ϕ' , and c are the vertical effective stress, the effective internal friction angle of soil, and the cohesion, respectively. This expression is known as Coulomb’s equation. The shear stress at peak state was considered as failure state. Rearranging Eq. (1), the internal friction angle is equal to ϕ' .

$$\phi' = \tan^{-1} \frac{(\tau - c)}{\sigma'_v} \tag{2}$$

In reference to Schofield and Wroth (1968), the critical state is a state at which the soil deforms plastically at the constant effective stress and void ratio, as illustrated in Fig. 2. The back analysis of the instability of earth structure indicates that the stress at the critical states is consistent with the stress at failure in the real site. At this state, the soil structure such as the interlocking (Taylor 1948) or the cementation from chemical bonding or soil mineral (Ohta et al. 2010; Schofield and Wroth 1968) is completely destructured. The cohesion becomes zero. Hence, the internal friction angle at the critical state becomes

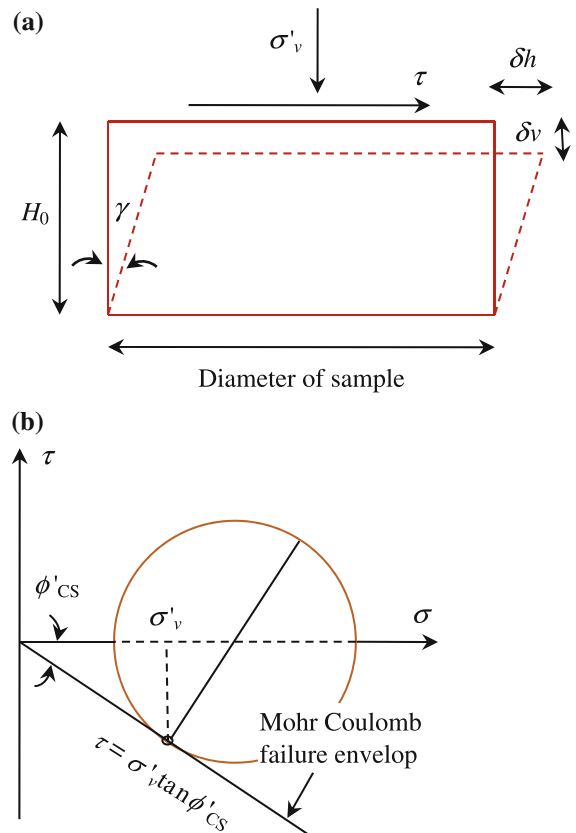


Fig. 1 Failure state occurred on horizontal plane from routine direct simple shear test. **a** Stress state drawn in physical space, and **b** stress state drawn in Mohr space (σ, τ)

$$\phi'_{CS} = \tan^{-1} \frac{\tau}{\sigma'_v} \tag{3}$$

Moreover, Luong (1980) defined the characteristic state (CH) state at which soil changes from compression to dilation as shown in Fig. 2a, c. Georgiannou et al. (2008) experimentally proved from torsional hollow cylinder test that this CH state in the drained test was to be equivalent to the phase transformation (PT) state in undrained condition in Fig. 2b, d at which the excess pore water pressure changes from positive to negative (Ishihara et al. 1975).

The critical state and PT state play a very important role in dynamic analysis involving the earthquake induced damage to the soil structures and foundations in saturated cohesionless soils (Castro 1975; Georgiannou et al. 2008; Porcino et al. 2008). Many researchers (Iai et al. 1992; Pender 1980; Ishihara and Towhata 1982) have developed various models to predict the effective stress paths for cyclic mobility

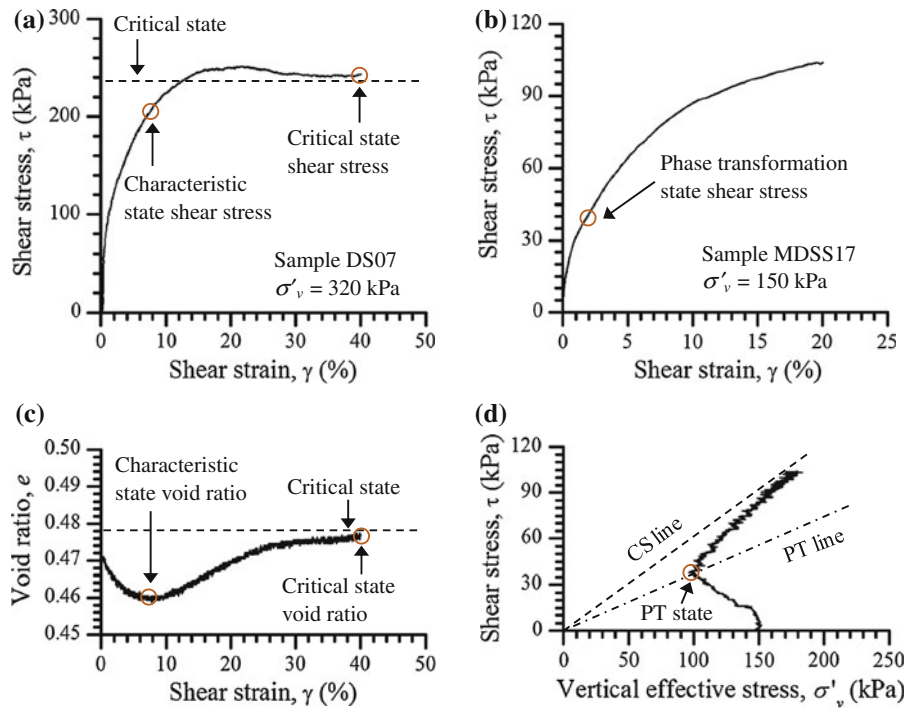


Fig. 2 Monotonic soil behavior under constant vertical stress condition **a** in (τ - γ) space and **b** in (e - γ) space, and under constant volume condition **c** in (τ - γ) space and **d** in (τ - σ'_v) space

induced by earthquake loading within a framework of critical state and PT state.

2.3 Dynamic Direct Simple Shear Test

Cyclic loading direct simple shear test is considered as a close laboratory simulation of the seismic ground shaking under the repeated horizontal shear force with reference to Seed et al. (1986). The shear modulus and the damping ratio are two of the key parameters of dynamic properties, which can be determined to evaluate ground response concerning no residual soil displacements under reasonably symmetrical cyclic loading condition.

Normally, the shear modulus is defined as the secant modulus calculated by the extreme points on the hysteresis loop, while the area inside the hysteresis loop gives an indication of the damping ratio of the soil. The configuration of hysteresis loop during cyclic loading is presented in Fig. 3. The shear modulus (G) and the damping ratio (λ) of a soil subjected to the simple shear cyclic loading from Fig. 3 can be simply expressed as

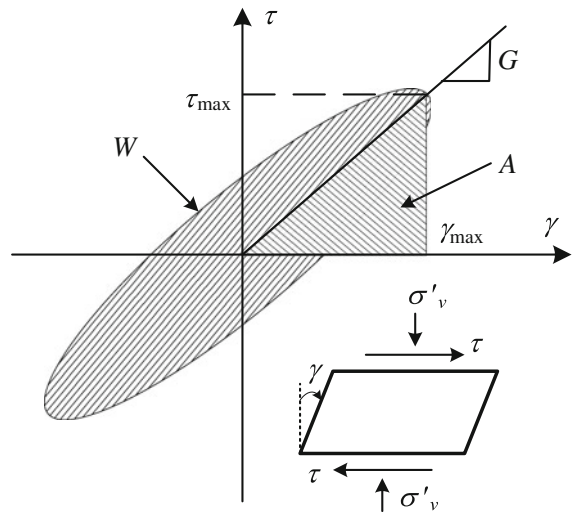


Fig. 3 Hysteretic stress–strain relationship during cyclic loading

$$G = \frac{\tau_{\max}}{\gamma_{\max}} \tag{4}$$

$$\lambda = \frac{1}{4\pi} \frac{W}{A} \tag{5}$$

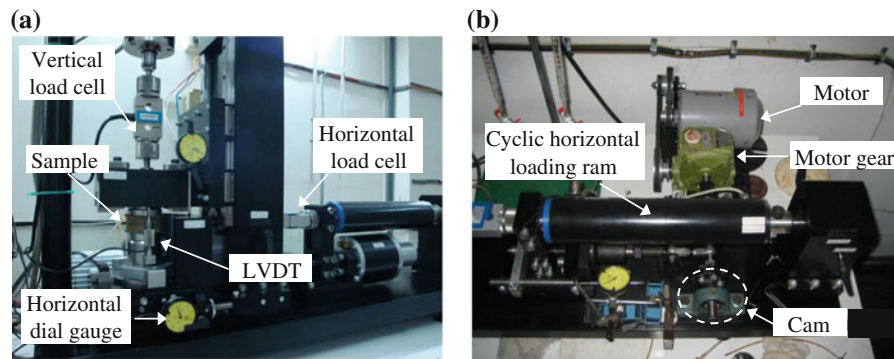


Fig. 4 NGI direct simple shear apparatus. **a** Monotonic DSS device, and **b** Mechanical device of cyclic control system

where τ_{max} , γ_{max} , and W are the maximum shear stress, the maximum shear strain amplitude, and the area of the hysteresis loop, respectively. The area (A) can be determined as

$$A = \frac{1}{2} \gamma_{max} \tau_{max} \quad (6)$$

According to the previous research carried out by various researchers (Iwasaki et al. 1978; Seed et al. 1986), the shear modulus and damping ratio are dependent of shear strain amplitude (γ), vertical stress (σ'_v), relative density (D_r), number of cycles (N), frequency (f), plasticity index (PI). The shape of the hysteresis loops observed during cyclic loadings is strongly influenced by the shear strain level due to the different induced soil behaviors. The shear modulus decreases with increasing shear strain amplitude. The shear modulus (G) characterizes that the loops decreases when the strain amplitude increases, whereas the damping ratio (λ) increases. At large stress cycles the grain structure continuously deteriorates, leading to a reduction of the soil resistance during each cycle. It results in a reduction of the shear modulus and of the damping ratio as a function of the number of cycles.

3 Experimental Program

3.1 Testing Apparatus

As shown in Fig. 4, the direct simple shear (DSS) apparatus developed by Bjerrum and Landva (1966) at the Norwegian Geotechnical Institute (NGI) is employed in the investigation to evaluate the static and dynamic properties of Chiang Mai sand. A cylindrical sample is laterally confined by a wire-reinforced membrane which is able to constrain lateral staining

and allows vertical deformation during consolidation and shear. The height and area of the sample are 16 mm and 35 cm². The vertical and horizontal load cells have the maximum capacity of 10 and 5 kN, respectively.

Monotonic NGI DSS apparatus in Fig. 4a was modified through the manual mechanical cyclic control system to permit cyclic strain controlled simple shear testing in this research, as presented in Fig. 4b. The mechanism of this cyclic control system is simple and easy to be operated. The three phase motor, which can be rotated in 3,400 rounds per minute, is used to apply the cyclic force by moving the horizontal loading ram back and forth. The motor gear of speed ratio 1:60 is also equipped to reduce the high speed of the motor. The cyclic shear strain amplitude can be set in a restricted range of 0.5–10 %, which is equal to 0.08–1.6 mm of horizontal displacement.

3.2 Physical Properties of Chiang Mai Sand

Figure 5 illustrates the typical subsoil profile in Chiang Mai province, northern part of Thailand, according to Pattarattanakul (2003). The tested sand specimen was taken from the Chiang Mai river bank, named Mae Ping, at latitude 18°78'N, and longitude 99°01'E. Mae Ping is situated in low to medium seismic risk zone. This river is the largest and most important river originating from the mountains of Chiang Dao and flowing southward for 540 km.

The particle size distribution curve of the CM sand after removal of particles greater than 4.75 mm is plotted as percentage passing against particle size, as depicted in Fig. 6. It can be seen that the CM sand consists of 5 % fine content and can be classified as poorly graded sand. Table 1 summarizes identification

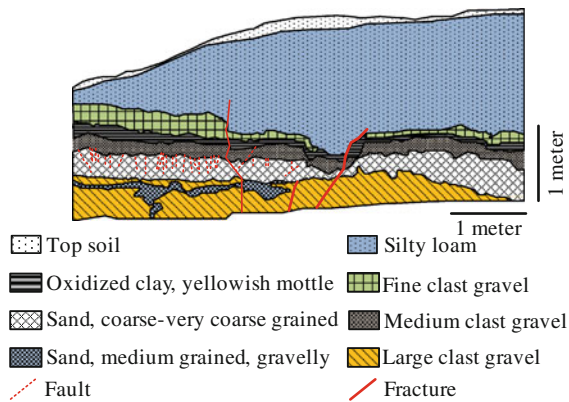


Fig. 5 Typical subsoil profile in Chiang Mai province, Thailand (Pattarattanukul 2003)

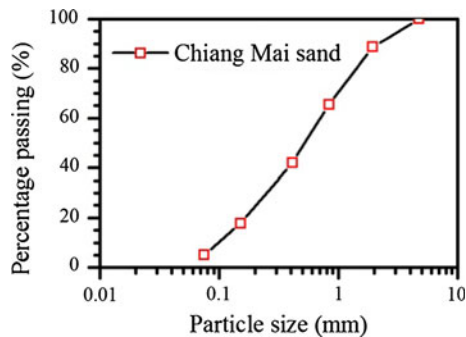


Fig. 6 Particle size distribution curve of CM sand

tests, including X-ray diffraction, grain size analysis, specific gravity measurement, and maximum and minimum void ratio (JIS A 1224). To determine maximum void ratio, the sand was filled in plastic funnel and dropped at zero height at the center of the cylindrical mould having 4-cm height and 6-cm diameter with speed from 20 to 30 s. The minimum void ratio can be obtained knocking around the mould a thousand hits using wood hammer within 200 s. The CM sand is greatly composed of 50 % quartz and 48 % Orthoclase according to the X-ray diffraction results. In addition, the tested sand was examined by

Table 1 Chiang Mai sand properties

Components of CM sand by X-ray diffraction			Physical properties of CM sand						
Quartz	Orthoclase	Muscovite	G_s^a	e_{min}^b	e_{max}^c	d_{50}^d	C_u^e	C_c^f	USCS ^g
50 %	48 %	2 %	2.62	0.400	0.806	0.52	7.48	0.92	SP

^a G_s is specific gravity; ^b e_{min} and ^c e_{max} are minimum and maximum void ratio (JIS A 1224); ^d d_{50} (mm) is median particle size; ^e C_u and ^f C_c are coefficients of uniform and curvature respectively; ^g USCS stands for the unified soil classification system

scanning electron microscope (SEM), as shown in Fig. 7. Sand and fine particles were viewed separately. Figure 7a points out that the sand particles were apparent to be rounded to sub-rounded, and it was likely from Fig. 7b that the flat and angular fine particles were attached to sand surface.

3.3 Sample Preparation Technique

The specimen is prepared by dry deposition technique in order to make sample uniform as to Ishihara (1993). The specimen is encased with the wire-reinforced membrane in direct simple shear (DSS) trimming tool. Oven-dry sand is filled into a cone-shaped plastic funnel with a nozzle of 12 mm in diameter, as shown in Fig. 8a. The funnel is moved up slowly at zero drop height with a speed ranging from 1.33 to 2 mm/s until the sand comes out completely from the funnel. The small seating load, as portrayed in Fig. 8b, was placed on top of the sample and the mold was tamped or hit at the bottom gently to obtain the very dense samples. After preparation, the sample is placed in DSS apparatus, and loaded to vertical stress desired for the test. The distilled water circulates through the sample from the bottom to the top followed by the carbon dioxide gas (CO_2) for 10 min in order to improve the saturation of the tested sample. The percolation of distilled water proceeds until the air bubbles disappears in the pipe connected to the sample top cap. The saturation of the samples varies within a range from 95 to 97 %, based on the water content of the samples after consolidation and before shearing and also at the end of the test by closing the drainage valves. The density of the sample after consolidation and before shearing can be assessed automatically from vertical displacement transducer.

3.4 Testing Program

A summary of the tests undertaken is given in Table 2. The monotonic direct simple shear test was conducted on CM sand under constant vertical stress (CL) and

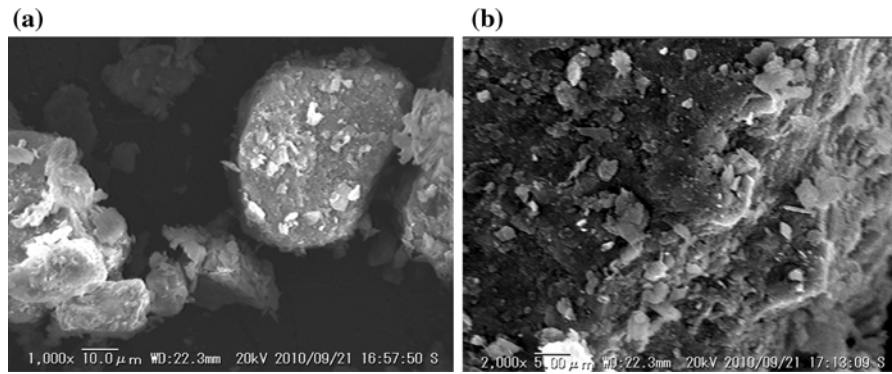


Fig. 7 Photo of CM sand from scanning electron microscope (SEM). **a** Round to sub-rounded sand particle (SEM photograph enlarged by $\times 1,000$), and **b** Flat fine particle on sand surface (SEM photograph enlarged by $\times 2,000$)

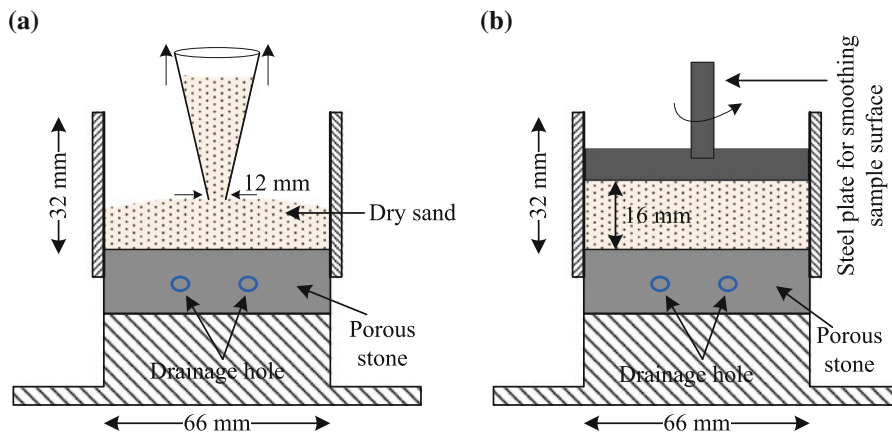


Fig. 8 Sample prepared by dry deposition technique on NGI DSS trimming tool. **a** Sand dropped through a plastic funnel, and **b** specimen smoothed on the top

constant volume (CV) condition, and the cyclic simple shear test under CL condition. The routine direct shear test is also carried out on CM sand samples prepared by dry deposition technique in addition to the direct simple shear test. Due to being reconstituted by dry deposition method, all samples are in dense state or in dry side of critical state, as described in Table 2. This is also noticed by Roscoe (1970). In order to investigate static and dynamic properties of CM sand, various vertical effective stresses and shear strain amplitudes are employed in this study. A quick shear rate of 0.1 mm/min was applied for monotonic shearing due to high permeability of sand. According to Peacock and Seed (1968), and Silver and Seed (1971), dynamic properties are found to be significantly unaffected by frequency in an approximate range of from 0.1 to 4 Hz. Therefore, a frequency of 0.1 Hz was chosen in the cyclic shearing.

The data obtained from direct simple shear and direct shear test in Table 2 are presented in terms of shear (γ) and vertical strain (ϵ_v) in order to be compared as follows:

$$\gamma = \frac{\delta h}{H_0} \tag{7}$$

$$\epsilon_v = \frac{\delta v}{H_0} \tag{8}$$

where δh and δv are the horizontal and vertical displacements and H_0 is the initial sample height.

4 Monotonic Simple Shear Behavior

The monotonic behavior of Chiang Mai Sand subjected to simple shear mode is investigated. In the testing program, a shear rate of 0.1 mm/min was

Table 2 A summary of testing program

Test type	Test no.	e_0	D_{r0} (%)	γ (%)	σ'_v (kPa)
Direct shear (DS)	DS01	0.493	77	–	40
	DS02	0.464	84	–	40
	DS03	0.506	74	–	80
	DS04	0.479	81	–	80
	DS05	0.473	82	–	160
	DS06	0.475	82	–	160
	DS07	0.471	83	–	320
	DS08	0.465	84	–	320
Monotonic CLDSS test	MDSS01	0.539	66	–	50
	MDSS02	0.517	71	–	50
	MDSS03	0.468	83	–	100
	MDSS04	0.556	61	–	100
	MDSS05	0.473	82	–	150
	MDSS06	0.525	69	–	150
	MDSS07	0.506	74	–	200
	MDSS08	0.498	76	–	200
Monotonic CVDSS test	MDSS09	0.505	74.26	–	50
	MDSS10	0.540	65.52	–	50
	MDSS11	0.482	79.81	–	100
	MDSS12	0.556	61.58	–	100
	MDSS13	0.487	78.57	–	150
	MDSS14	0.560	60.59	–	150
	MDSS15	0.465	83.99	–	200
	MDSS16	0.545	64.29	–	200
Cyclic direct simple shear test	CDSS01	0.525	69	0.5	100
	CDSS02	0.538	66	0.5	200
	CDSS03	0.529	68	0.5	300
	CDSS04	0.539	66	1	100
	CDSS05	0.525	69	1	200
	CDSS06	0.539	66	1	300
	CDSS07	0.529	68	2	100
	CDSS08	0.525	69	2	200
	CDSS09	0.529	68	2	300
	CDSS10	0.441	90	0.5	100
	CDSS11	0.454	87	0.5	200
	CDSS12	0.435	91	0.5	300
	CDSS13	0.441	90	1	100
	CDSS14	0.435	91	1	200
	CDSS15	0.454	87	1	300
	CDSS16	0.441	90	2	100
	CDSS17	0.441	90	2	200
	CDSS18	0.433	92	2	300

e_0 is initial void ratio before shearing, corresponding to initial relative density D_{r0}

applied during shear. The stress strain behavior of a series of tests on three samples (MDSS04, MDSS0405, and MDSS07) are illustrated in Fig. 9 plotted as shear stress (τ) and vertical strain (ϵ_v) against shear strain (γ). The positive and negative signs in Fig. 9b signify compression and expansion of samples, respectively, during the shearing stage. These samples have initial relative densities before shearing (after vertical effective stress applied) $D_{r,0} = 61, 82,$ and 74% with vertical effective stress, $\sigma'_v = 100, 150$ and 200 kPa, respectively. It is apparent from Fig. 9a that all the samples undergo two stages: First, the samples reach failure at peak shear stress in the range of shear strain from 7 to 11 %. Second, the peak shear stress slightly decreases with increasing volume, as illustrated in Fig. 9b, to the almost constant shear stress and constant volume at large shear strain $\gamma = 25\%$. It seems probable that the foregoing samples reach reasonable critical states although there is still a small variation of volumetric strain at the end of the test at approximate shear strain $\gamma = 25\%$. This agrees with previous finding by Atkinson et al. (1991), Ishihara (1993), and Verdugo and Ishihara (1996). The critical state was assumed to be approximately attained at shear strain $\gamma = 25\%$ in reference to their experimental data obtained from the direct simple shear apparatus under the constant vertical stress condition.

The comparison is made between direct simple shear (DSS) and direct shear (DS) test, as presented in Fig. 10. Two samples (MDSS03 and MDSS08) from the constant vertical stress DSS test and the other two samples (DS04 and DS05) from the standard DS test are selected to observe the discrepancy in strength behavior. It is clear from Fig. 10a, c that the samples from DS test require larger shear strain to reach reasonable critical state. Besides, in order to compare the values of CM sand strength from the two tests mentioned above, the stress ratio (τ/σ'_v) are plotted against shear strain (γ), as shown in Fig. 10b, d. The result points out that stress ratio at peak and critical state from DS test give higher value than those obtained from DSS test. This might be due to non-uniformity of deformation and stress distribution during shear, with reference to Kjellman (1951). Additionally, Fig. 10d depicts the evolution of mobilized friction angle (ϕ'), calculated as $\tan^{-1}(\tau/\sigma'_v)$ during shear of DSS and DS test. At the critical state, the mobilized friction angle (ϕ'_{CS}) of

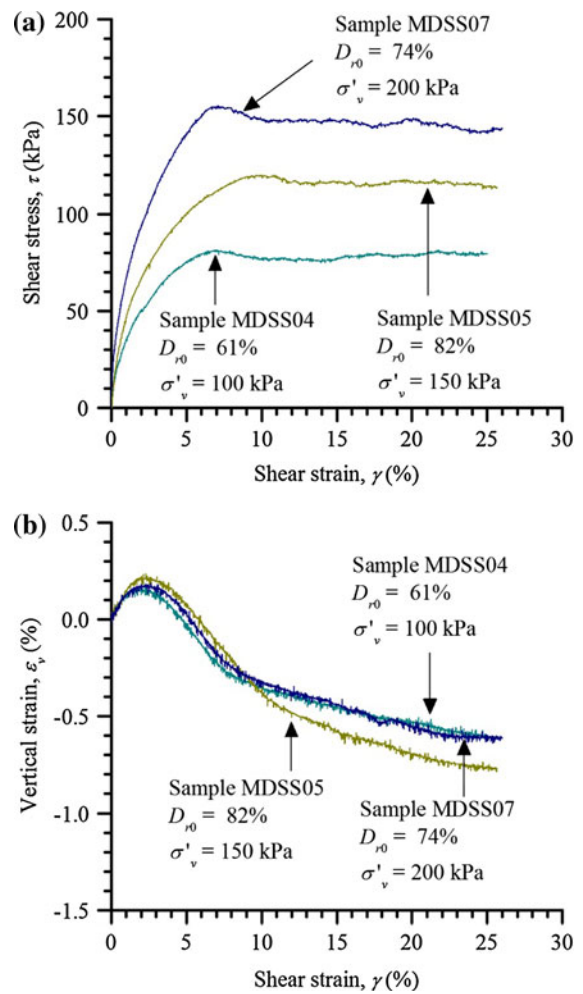
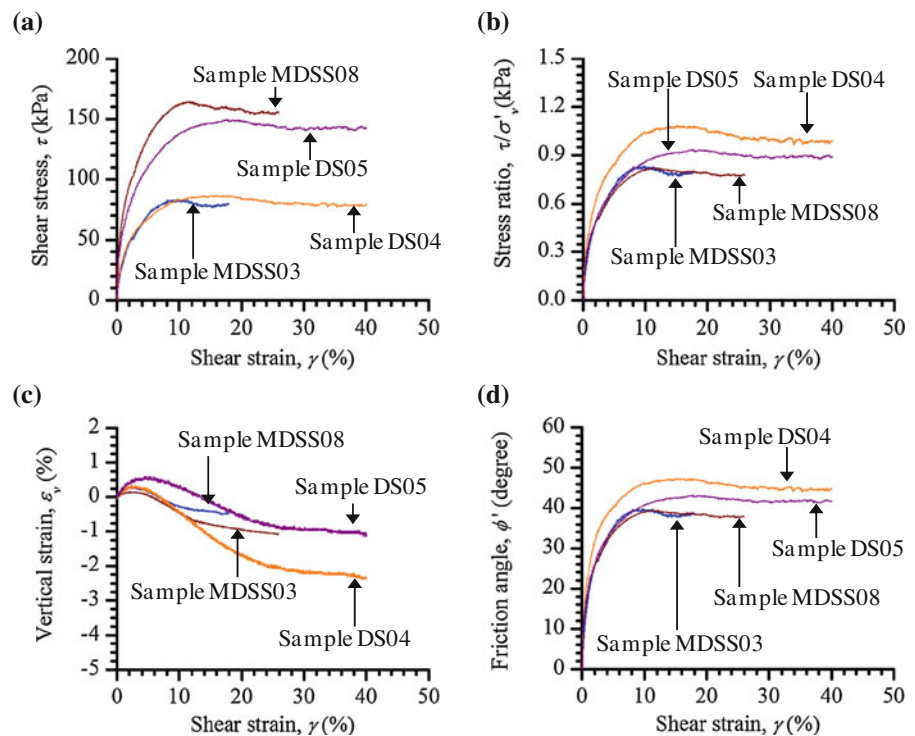


Fig. 9 Monotonic simple shear behavior of Chiang Mai sand of three samples at different vertical effective stresses $\sigma'_v = 100, 150$ and 200 kPa. **a** Stress strain behavior, and **b** volumetric strain behaviour

samples MDSS03 and MDSS08 from DSS test was found to be approximately equal. On the contrary, the ϕ'_{CS} of samples DS04 and DS05 from DS test seems to be different.

The critical (CS) state, the characteristic (CH) state, and the PT state in (τ, σ'_v) space from the constant vertical stress and constant volume monotonic direct simple shear (CLDSS) and (CVDSS) test, and direct shear (DS) test are shown in Fig. 11 plotted as shear stress against vertical effective stress. Figure 11a points out that all the data of the test series from DSS test in the present study are in good consistency, forming a unique critical state (CS) line with zero cohesion intercept. This also accords fully with the

Fig. 10 Comparison of CM sand behavior under simple shear mode and direct shear mode. **a** Stress strain behavior, **b** normalized stress strain behavior, **c** volumetric strain behavior, and **d** mobilized internal friction angle



previous studies of DSS test carried out by Roscoe et al. (1958) on glass beads and steel balls. Nevertheless, the data from another series of test results obtained from standard DS test seems slightly scattered around a unique CS line. This might be due to the non-uniformity of stress and strain distribution, as discussed in Sect. 2. It could explicitly be concluded from Fig. 11a, b that the internal friction angle mobilized at the CS state from CLDSS test and CVDSS test was found at $\phi'_{CS}(\text{CLDSS}) = 37.3^\circ$ and $\phi'_{CS}(\text{CVDSS}) = 30^\circ$, in which was 9 and 26.8 % less than that from DS test ($\phi'_{CS}(\text{DS}) = 41^\circ$). In addition, Fig. 11c, d shows that the CH state shear stress obtained from CLDSS test in this study lies on the straight line, in which $\phi'_{CH}(\text{CLDSS}) = 26.7^\circ$ is 3.7° higher than the friction angle at the PT state from CVDSS test ($\phi'_{PT}(\text{CVDSS}) = 23^\circ$) and 8.8° lower than the friction angle at the CH state from DS test ($\phi'_{CH}(\text{DS}) = 35.5^\circ$).

5 Cyclic Simple Shear Behavior

The cyclic shear stress induced in the ground during an earthquake is caused by the upward propagation of shear waves. In many cases, the vertical stress exerting to the

soil element keeps constant while the cyclic shear stress imposed on the element reverse direction for many times; hence, the monotonic and cyclic direct simple shear test was conducted on saturated sample under constant vertical stress condition. The specimen was prepared by dry deposition technique in order to make sample uniform, according to Ishihara (1993). The 18 samples were tested at different vertical stresses (σ'_v), amplitude shear strains (γ), and initial relative densities before shearing (D_{r0}), as shown in Table 2. Based on Silver and Seed (1971), the dynamic soil response is unaffected by frequency. As a result, $f = 0.1$ Hz is chosen to conduct the experiment in this study.

The evolution of hysteresis loop of cyclic DSS test on sample CDSS07 at different number of cycles is illustrated in Fig. 12 plotted as shear stress against shear strain. This sample undergoes the shear strain amplitude $\gamma = 0.5$ %, the vertical stress $\sigma'_v = 100$ kPa and relative density $D_{r0} = 68$ %. As discussed earlier, the shear modulus (G) can be determined by the extreme points on the hysteresis loop, while the area inside the hysteresis loop is described by the damping ratio (λ) of the soil. It is apparent from Fig. 12 that the shear modulus and damping ratio depends on the number of cycles during cyclic direct simple shear test. The slope of the hysteresis loop becomes higher

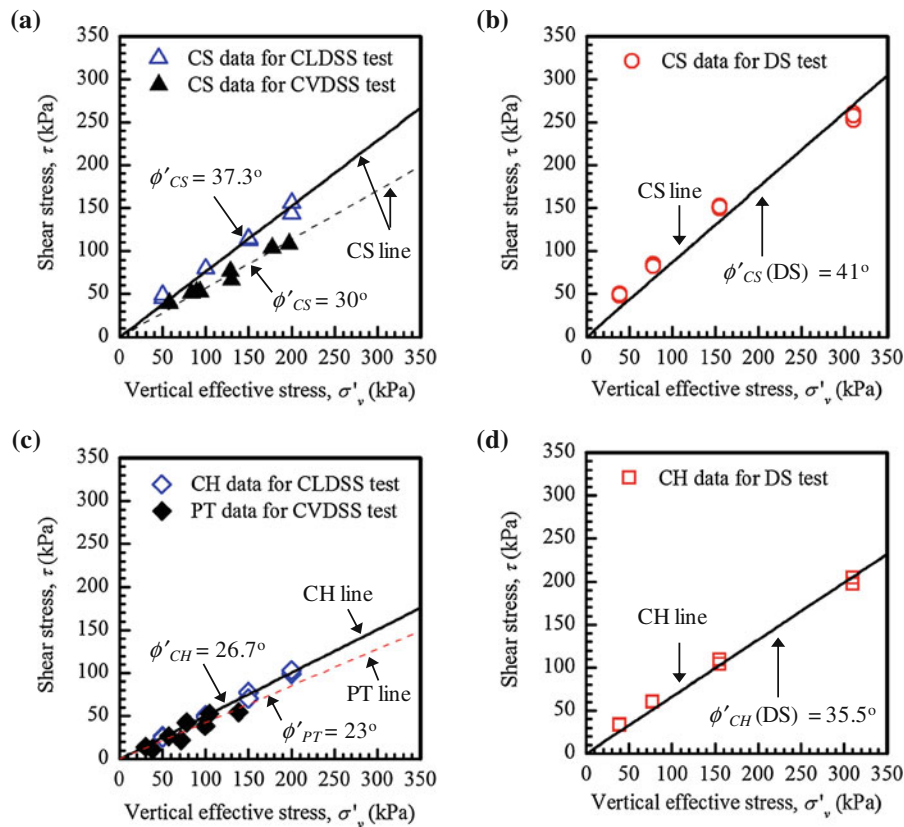


Fig. 11 Stress path behavior in (τ, σ'_v) space **a** CS state from CLDSS and CVDSS test, **b** at CS state from DS test, **c** at CH state and PT state from CLDSS test and CVDSS test, and **d** at CH state from DS test

and the area of the loop becomes smaller. As calculated in accordance with Eqs. (4) and (5), the shear modulus increases from 2.82 to 4.79 MPa with increasing number of cycles from 10 to 1,000 cycles.

5.1 Shear Modulus of Chiang Mai Sand under Cyclic Direct Simple Shear Mode

Figure 13 presents the effect of the vertical stress and the shear strain amplitude on the shear modulus of CM sand at different number of cycles $N = 10$ th cycle and 1,000th cycle for samples CDSS01-09 with approximate initial relative density $D_{r0} \cong 68\%$. The shear modulus (G) was plotted against shear strain amplitude (γ). The symbols of rectangle, circle, and triangle represent the samples subjected to the vertical stress $\sigma'_v = 100, 200, \text{ and } 300$ kPa. Figure 13a clearly indicates that there is a decrease in shear modulus (G) with increasing shear strain amplitude (γ) at $N = 10$ th cycle in the entire range of the vertical stress

(σ'_v). It can also be noticed that the higher the vertical stress (σ'_v), the lower the fitted curve of the shear strain (γ). The effect of the vertical stress (σ'_v) on the shear modulus (G) seems to be small as σ'_v gets higher. Similar data and trends of the shear modulus for the same sample (CDSS01-09) at $N = 1,000$ th cycle, as shown in Fig. 13b, strongly confirm the foregoing observation at $N = 10$ th cycle for tests in Fig. 13a. Besides, the increase of N in a range of 10th cycle to 1,000th cycle on $-\gamma$ relationship in Fig. 13a and b is likely to be small on the shear modulus. The samples CDSS10-18 were found to show the similar trend as samples CDSS01-09. This is in good agreement with Silver and Seed (1971) that the value of G seems to be similar after $N = 10$ th cycle. This is the reason why many researchers would like to select $N = 10$ th cycle to investigate the cyclic soil response.

The direct simple shear test was conducted under the constant vertical stress condition, which is equivalent to the drained test. The density of sample increases

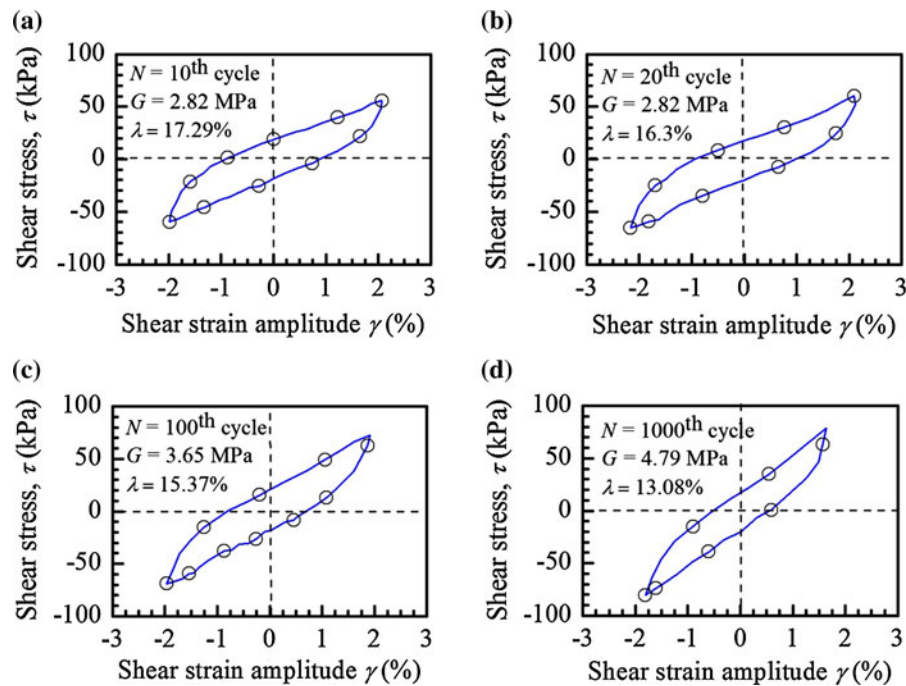


Fig. 12 Hysteresis loop of cyclic DSS test on sample CDSS07 at different number of cycles. **a** At 10th cycle, **b** at 20th cycle, **c** at 100th cycle, and **d** at 1,000th cycle

during cyclic loading from one cycle to another cycle. In this paper, the effect of initial relative density before shearing (D_{r0}) subjected to the cyclic loading was investigated. Figure 14 shows the shear modulus data of the samples at $N = 10$ th cycle and $\sigma'_v = 300$ kPa. The solid and dot curve are fitted with the data of the samples having $D_{r0} \cong 68$ and 90 %. Figure 14 can be pointed out that the shear modulus at $N = 10$ th cycle slightly increase as the sample is denser. The values of modulus seem not to be much affected by initial relative density $D_{r0} \cong 68$ and 90 % in the entire range of the shear strain employed in this study.

5.2 Damping Ratio of Chiang Mai Sand under Cyclic Direct Simple Shear Mode

After an interpretation of the shear modulus from constant vertical stress cyclic DSS test in previous section, the results of viscous damping ratio will be interpreted and analyzed. Comparison of these experimental results will be illustrated in the following section. Hysteretic damping ratio (γ) is plotted against number of stress cycles (N) in the cyclic direct simple shear test carried out on sample CDSS02, 08 and 14 at $\sigma'_v = 200$ kPa, as shown in Fig. 15. It can be seen that the value of the damping λ

decreases with increasing N for the range of the shear strain amplitude in the testing program.

Relationship between hysteretic damping and shear strain amplitude of CM sand is presented in Fig. 16. The samples with approximate initial relative density $D_{r0} \cong 68$ and 90 % are plotted together in order to observe their effect on damping ratio. Figure 16a points out that the values of damping are likely to be independent of the D_{r0} at $N = 10$ th cycle for all practical purposes. Similar trends can be seen in Fig. 16b at $N = 1,000$ th cycle. In addition, it can be observed that there is a decrease in λ with increasing γ in the entire range of σ'_v selected in the research study. For a given γ , calculated values of damping ratio (λ) decreases as vertical stress (σ'_v) increases. The tendency to reduce damping ratio is important for ground shaking analysis. It is usually convenient to use an average damping ratio in $N = 10$ th cycle according to Seed et al. (1986).

6 Discussion

While the measured shear modulus and damping ratio values obtained from DSS test are consistent in

Fig. 13 Relationship between shear modulus and shear strain amplitude of CM sand **a** at $N = 10$ th cycle and **b** 1,000th cycle for sample CDSS01-09

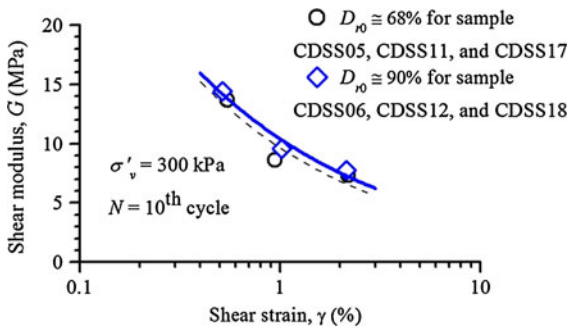
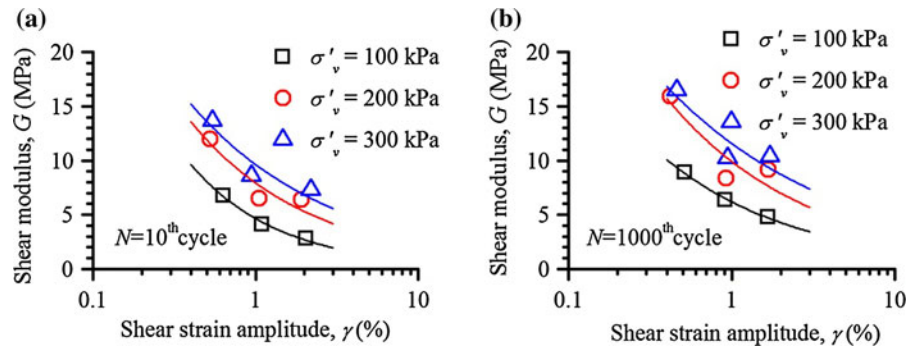


Fig. 14 Effect of initial relative density (D_{r0}) on the shear modulus

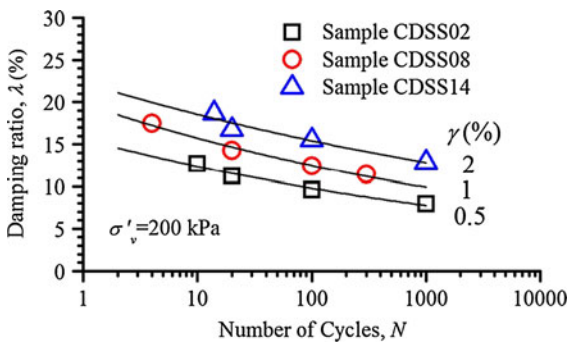


Fig. 15 Characteristics of damping for samples CDSS11, CDSS14, and CDSS18 at $\sigma'_v = 200$ kPa

themselves, it is of interest to compare the testing results with values obtained by other investigators using different techniques. Such a comparison is shown in Figs. 17 and 18.

Figure 17 presents the shear modulus of Chiang Mai sand in the present study in comparison with that of Toyoura sand measured by Iwasaki et al. (1978). The ratio of the shear modulus (G) versus the maximum modulus (G_{max}) was plotted against the shear strain amplitude in the wide range from 10^{-6} to 10 % at the number of stress cycle $N = 10$ th cycle. Triangle and

diamond represent a series of samples tested in the program at $D_{r0} \cong 68$ and 90 % for $\sigma'_v = 300$ kPa. For the sake of the simplicity of the comparison, Jaky's formula has been adopted to calculate the lateral earth pressure at rest with the friction angle of 37.3° . Thus, the effective vertical stress $\sigma'_v = 300$ kPa can be computed to the mean effective stress $p' \cong 180$ kPa. In addition, in order to be compared with the previous study, the data of the Chiang Mai sand modulus in the present study was normalized by the in situ maximum shear modulus. This shear modulus can be estimated by shear wave velocity (v_s) from the multichannel analysis of surface wave (MASW) method at the same location (Seng 2008): $G_{max} = \gamma v_s^2 / g$ where $\gamma =$ unit weight of the soil and $g =$ gravity. The effective vertical stress $\sigma'_v = 300$ kPa is approximately equal to 20 m depth at the site because the water table level is 10 m below the soil surface and the density of sand at this depth about $\gamma = 20$ kN/m³, thus giving $v_s = 261$ m/s² (Seng 2008), which corresponds to $G_{max} = 136$ MPa.

It is apparent from Fig. 17 that the normalized shear modulus from the DSS test is noticeably smaller than that from the resonant-column test and torsional shear test conducted by Iwasaki et al. (1978). The reason is the big gap of shear strain employed between the present and previous study. As discussed earlier, the modulus of any soil was greatly affected by the strain level induced in the sand according to Iwasaki et al. (1978), and Seed et al. (1986). Figure 17 also points out that for $p' \cong 180$ kPa the normalized modulus at large shear strain seems to lie around the dashed line while the normalized modulus at very small or small shear strain should be located around solid line proposed by Iwasaki et al. (1978).

In addition to the comparison of shear modulus, the direct simple shear results of the damping ratio in the

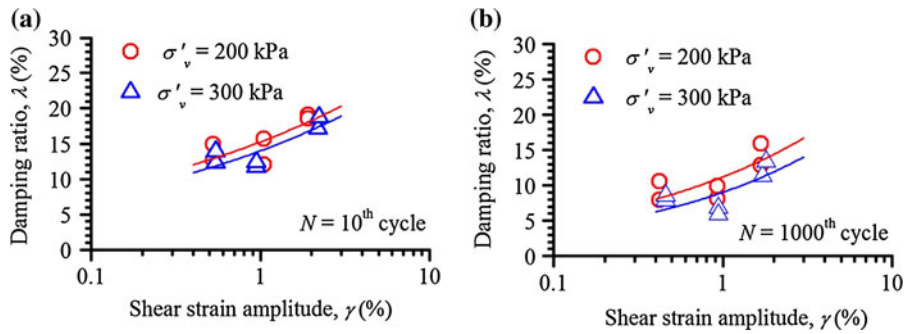


Fig. 16 Relationship between hysteretic damping and shear strain amplitude of CM sand for tested samples subjected to $\sigma'_v = 200$ and 300 kPa **a** at $N = 10^{\text{th}}$ cycle, and **b** at $N = 1,000^{\text{th}}$ cycle

Fig. 17 Comparison between shear modulus of Chiang Mai sand and Toyoura sand

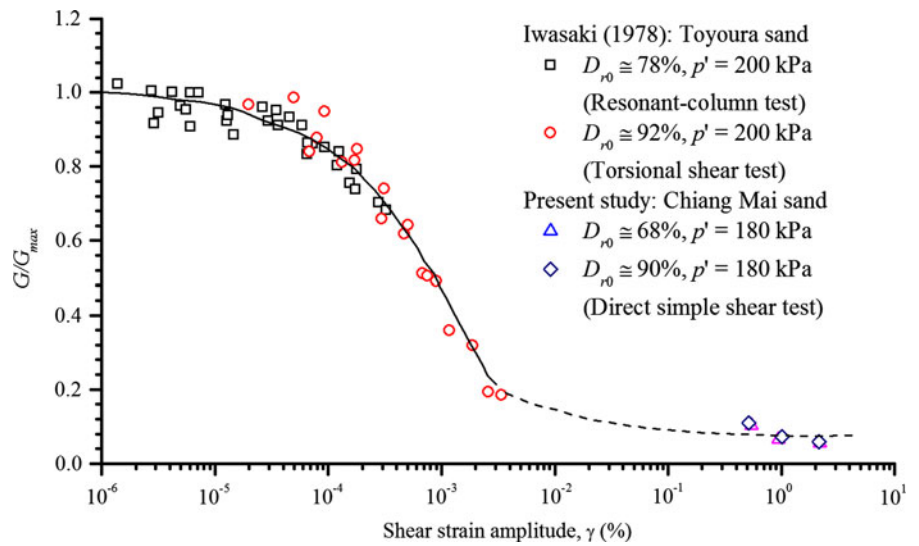


Fig. 18 Comparison between damping ratio of Chiang Mai sand and other researchers

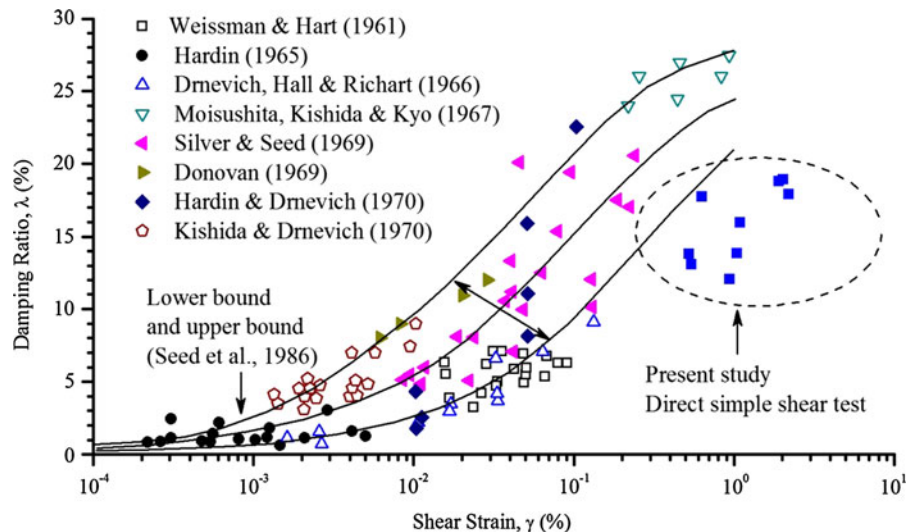


Table 3 Summary of dynamic properties of Chiang Mai sand at $N = 10^{\text{th}}$ cycle

Amplitude shear strain γ (%)	Vertical effective stress σ'_v (kPa)	Shear modulus G (MPa)	Damping ratio λ (%)
0.5	100	8.07	16.64
	200	11.85	12.65
	300	13.56	11.55
1	100	4.72	17.39
	200	7.94	15.87
	300	9.72	12
2	100	2.67	18.19
	200	5.26	18.28
	300	6.87	16.87

testing program were plotted in Fig. 18. As portrayed in Sect. 5.2, the relative density after $N = 10^{\text{th}}$ cycle has small effect on damping. Thus, the solid rectangle data in the present study are shown in the average values of damping at $D_{r0} \cong 68$ and 90 %, as illustrated in Fig. 18. The comparison can be made with the proposed range of the damping data for sand by Seed et al. (1986). All kinds of sands regardless of particle size and relative density will be in this assumed range. However, it can be seen from Fig. 18 that the data of the damping in the current study remains a bit lower than the lower bound suggested by Seed et al. (1986). This might be because of the lower bound by Seed et al. (1986) based on fitting the data points at the low strain level.

7 Conclusions

The behavior of the Chiang Mai sand was investigated through monotonic and cyclic direct simple shear tests. The results of the present study represent the dynamic characteristic of soil in the intermediate to large strain amplitude (shear strain of 0.5–2 %) and not small strain. The main conclusion drawn from the experimental result in the present study can be summarized as follows:

(a) The critical states can be reasonably determined from monotonic direct simple shear at approximate shear strain $\gamma = 25$ % although there is still a small variation of volumetric strain at the end of the test.

- (b) The internal friction angle mobilized at the critical state from direct simple shear test was found to be equal to ϕ'_{CS} (DSS) = 37.3°, which was 9 % less than that from direct shear test. This means that for practical design, the shear strength from DSS test is more conservative than that from the direct shear test.
- (c) The PT state shear stress in the present study lies on the straight line with slope ϕ'_{PT} (DSS) = 26.7° for direct simple shear test and ϕ'_{PT} (DS) = 35.5° for direct shear test.
- (d) According to Table 3, the maximum value of shear modulus and damping ratio at 10th cycle can be approximately equal to 13.56 MPa and 18.28 %, respectively within a range of shear strain from 0.5 to 2 % and of vertical stress from 100 to 300 kPa.
- (e) This paper also provides the relationship of the appropriate dynamic properties of Chiang Mai sand with the shear strain level < 2 % for any practical purpose. It is noted that the normalized shear modulus in the present study shows a good consistency with other investigators while the damping ratio is noticeably smaller than the lower-bound range for sand proposed by the previous study.

Acknowledgments Authors greatly appreciate Mr. Nirut Konkong and Mr. Piroj Anasetakul for their assistance with the modification of the cyclic control system for direct simple shear apparatus. The first author gratefully acknowledges the scholarship of the master and doctoral degree programs provided by Japan International Cooperation Agency (JICA) through the AUN/SEED-Net program. The second author would like to appreciate the overseas research grant 2009 from the Asahi Glass Foundation.

References

- Atkinson J, Lau WHW, Powell JJM (1991) Measurement of soil strength in simple shear tests. *Can Geotech J* 28:255–262
- Bjerrum L, Landva A (1966) Direct simple shear tests on a Norwegian quick clay. *Géotechnique* 16(1):1–22
- Budhu M (1988) Failure state of a sand in simple shear. *Can Geotech J* 25:395–400
- Castro G (1975) Liquefaction and cyclic mobility of saturated sand. *J Geotech Eng Div ASCE* 101(GT6):551–569
- Gauchan J (1984) Liquefaction tests on sand using a cyclic triaxial apparatus. Asian Institute of Technology, Bangkok
- Georgiannou VN, Tsomokos A, Stavrou K (2008) Monotonic and cyclic behaviour of sand under torsional loading. *Géotechnique* 58(2):113–124

- Iai S, Matsunaga Y, Kameoka T (1992) Strain space plasticity model for cyclic mobility. *Soils Found* 32(2):1–15
- Ishihara K (1993) Liquefaction and flow failure during earthquake. *Géotechnique* 43(3):351–415
- Ishihara K, Towhata I (1982) Dynamic response analysis of level ground based on the effective stress method. In: Pande GN, Zienkiewicz OC (eds) *Soil Mechanics-transient and cyclic loads*. Wiley, New York, pp 133–172
- Ishihara K, Tatsuoka F, Yasuda S (1975) Undrained deformation and liquefaction of sand under cyclic stresses. *Soils Found* 15(1):29–44
- Iwasaki T, Tatsuoka F, Takagi Y (1978) Shear moduli of sands under cyclic torsional shear loading. *Soils Found* 18(1):40–56
- Japanese Standards and Explanations of Laboratory Tests of Geomaterials (2000) JIS a 1224: test method for minimum and maximum densities of sands, 1st revision. Jpn Geotech Soc. ISBN:4-88644-058-4
- Kjellman W (1951) Testing the shear strength of clay in Sweden. *Géotechnique* 2(3):225–235
- Luong MP (1980) Stress-strain aspects of cohesionless soils under cyclic and transient loading. In: Pande GN, Zienkiewicz OC (eds) *International symposium on soils under cyclic and transient loading*. A.A. Balkema, Rotterdam, Netherlands, pp 315–324
- Nutalaya P, Sodsri S, Arnold EP (1985) Series on seismology. Paper presented at the Southeast Asia Association of Seismology and Earthquake Engineering, Bangkok, Thailand
- Ochiai H (1981) A method for calculating the undrained strength ratio, c_u/p , of normally consolidated clay measured in the simple shear test. *Soils Found* 21(1):109–115
- Ohta H, Pipatpongsa T, Heng S, Yokota S, Takemoto M (2010) Significance of saturated clays seams for the stability of rainfall-induced landslides. *Bull Eng Geol Environ* 69(1):71–87
- Ornthammarath T, Warnitchai P, Worakanchana K, Zaman S, Sigbjörnsson R, Lai C (2011) Probabilistic seismic hazard assessment for Thailand. *Bull Earthq Eng* 9(2):367–394. doi:10.1007/s10518-010-9197-3
- Pailoplee S, Sugiyama Y, Charusiri P (2009) Probabilistic seismic hazard analysis in thailand and adjacent areas by using regional seismic zones. *Terr Atmos Ocean Sci* 21(5):757–766
- Pattararattanakul P (2003) Liquefaction resistance of sands in the northern part of Thailand. Chulalongkorn University, Bangkok
- Peacock WH, Seed HB (1968) Sand liquefaction under cyclic loading simple shear conditions. *J Soil Mech Found Div ASCE* 94(SM3):689–708
- Pender MJ (1980) Cyclic mobility—a critical state model. Paper presented at the International Symposium on Soils under Cyclic and Transient Loading, Swansea
- Porcino D, Caridi G, Ghionna VN (2008) Undrained monotonic and cyclic simple shear behaviour of carbonate sand. *Géotechnique* 58(8):635–644
- Roscoe KH (1970) The influence of strains in soil mechanics—Tenth rankin lecture. *Géotechnique* 20(2):129–170
- Roscoe KH, Schofield AN, Wroth CP (1958) On the yielding of soils. *Géotechnique* 08(01):22–53
- Schofield AN, Wroth P (1968) *Critical state soil mechanics*. McGraw-Hill, London
- Seed HB, Wong RT, Idriss IM, Tokimatsu K (1986) Moduli and damping factors for dynamic analyses of cohesionless soils. *J Geotech Eng* 112(11):1016–1032
- Seng S (2008) Application of multichannel analysis of surface wave to shallow site investigation for subsoil in Thailand. Chulalongkorn University, Bangkok
- Silver ML, Seed HB (1971) Deformation characteristics of sands under cyclic loading. *J Soil Mech Found Div ASCE* 97(SM8):1081–1098
- Taylor DW (1948) *Fundamentals of soil mechanics*. Wiley, New York
- Teachavorasinskun S, Teachavorasinskun S, Pongvithayapranu P (2009) Liquefaction susceptibility in the Northern provinces of Thailand. *Am J Eng Appl Sci* 2(1):194–201
- Verdugo R, Ishihara K (1996) The steady state of sandy soils. *Soils Found* 36(2):81–91